QCD for (future) hadron colliders

ICTP Summer School

June 15- 26 2015

Lecture 2

Michelangelo L. Mangano

TH Unit, Physics Department, CERN

michelangelo.mangano@cern.ch

A useful ref:

Hard Interactions of Quarks and Gluons: a Primer for LHC Physics

http://arXiv.org/abs/hep-ph/0611148

Evolution of hadronic final states

Asymptotic freedom implies that at E_{CM} >> 1 GeV

$\sigma(e^+ e^- \to \text{hadrons})$ ⟷ $\sigma(e^+ e^- \to \text{quarks/gluons})$

At the Leading Order (LO) in PT:

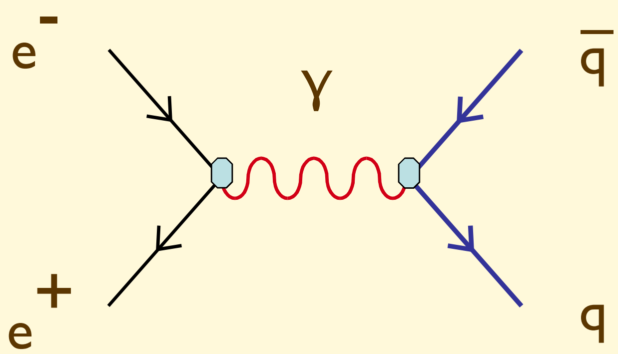

$$\sigma_0(e^+e^- \to q\bar{q}) = \frac{4\pi\alpha^2}{9s} N_c \sum_{f=u,d,\ldots} e_{q_f}^2$$

$$\frac{\sigma_0(e^+e^- \to q\bar{q})}{\sigma_0(e^+e^- \to \mu^+\mu^-)} = N_c \sum_{f=u,d,\ldots} e_{q_f}^2$$

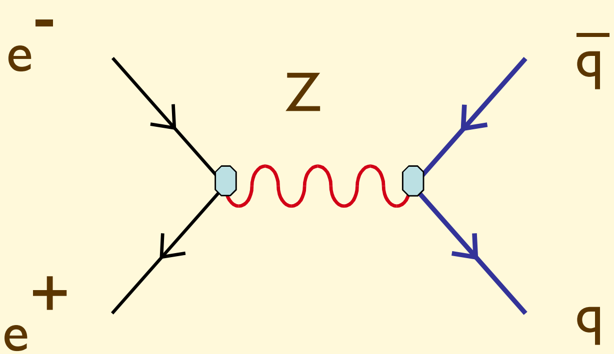

$$\frac{\sigma_0(e^+e^- \to Z \to q\bar{q})}{\sigma_0(e^+e^- \to Z \to \mu^+\mu^-)} = N_c \frac{\sum_{f=u,d,\ldots}\left(v_{q_f}^2 + a_{q_f}^2\right)}{\left(v_\mu^2 + a_\mu^2\right)}$$

Adding higher-order perturbative terms:

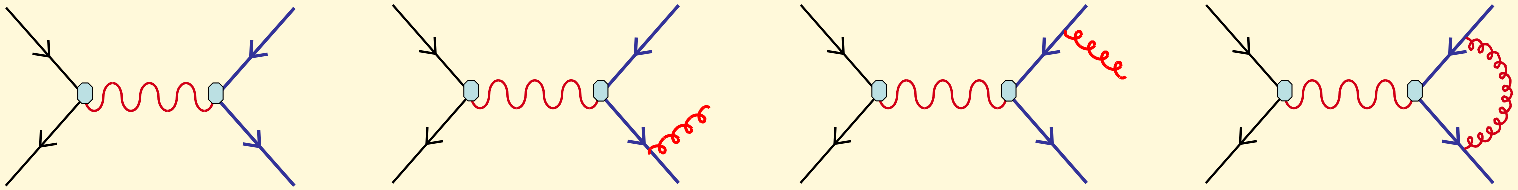

+ $\geq$2-gluon emissions

$$\sigma_1(e^+e^- \to qq(g)) = \sigma_0(e^+e^- \to qq)\left(1 + \frac{\alpha_s(E_{CM})}{\pi} + O(\alpha_s^2)\right)$$

O(3%) at M_Z

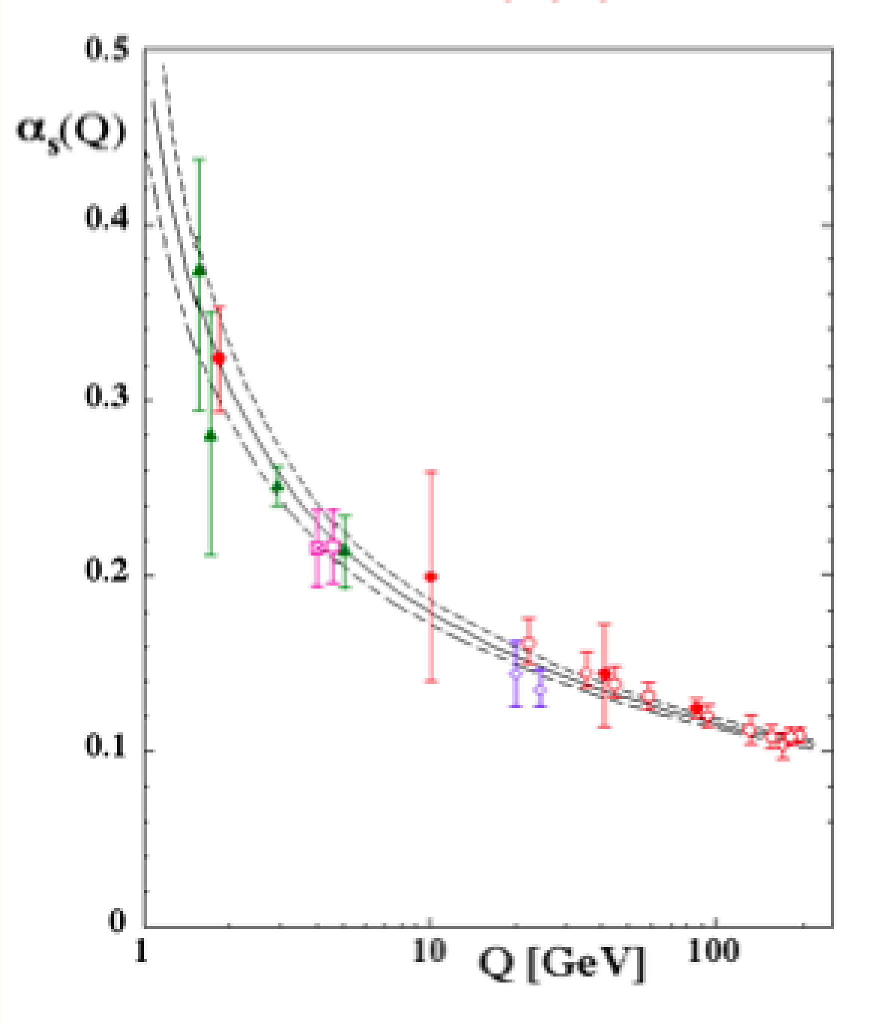

Excellent agreement with data,
provided N_c=3
Extraction of αs consistent with the Q evolution predicted by QCD

Experimentally, the final states contain a large number of particles, not the 2 or 3 that apparently saturate the perturbative cross-section.

Experimental multiplicity distribution

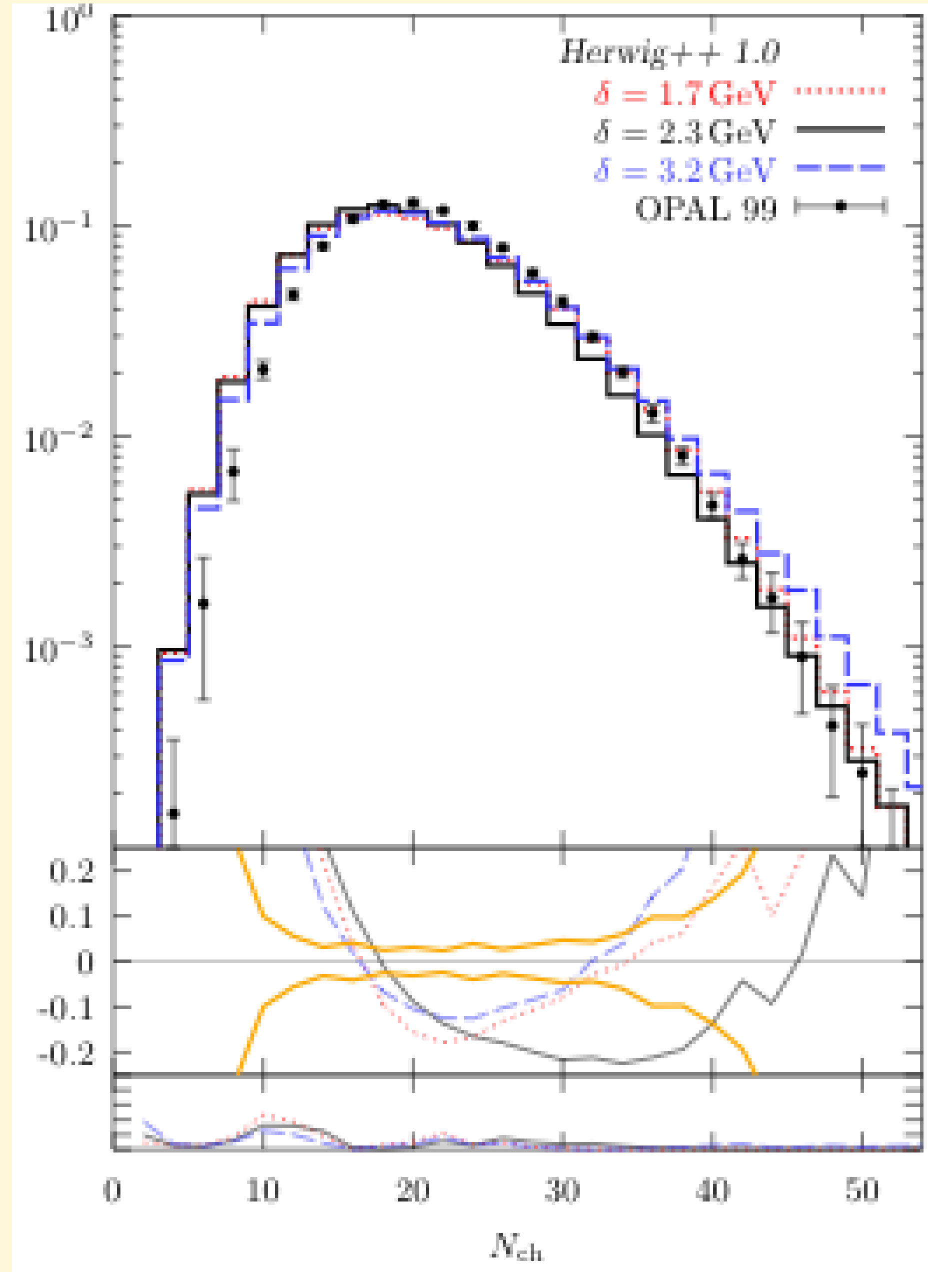

$\langle n_{charged} \rangle = 20.9$

Isn't this bizarre?

Look more closely at the structure of these events:

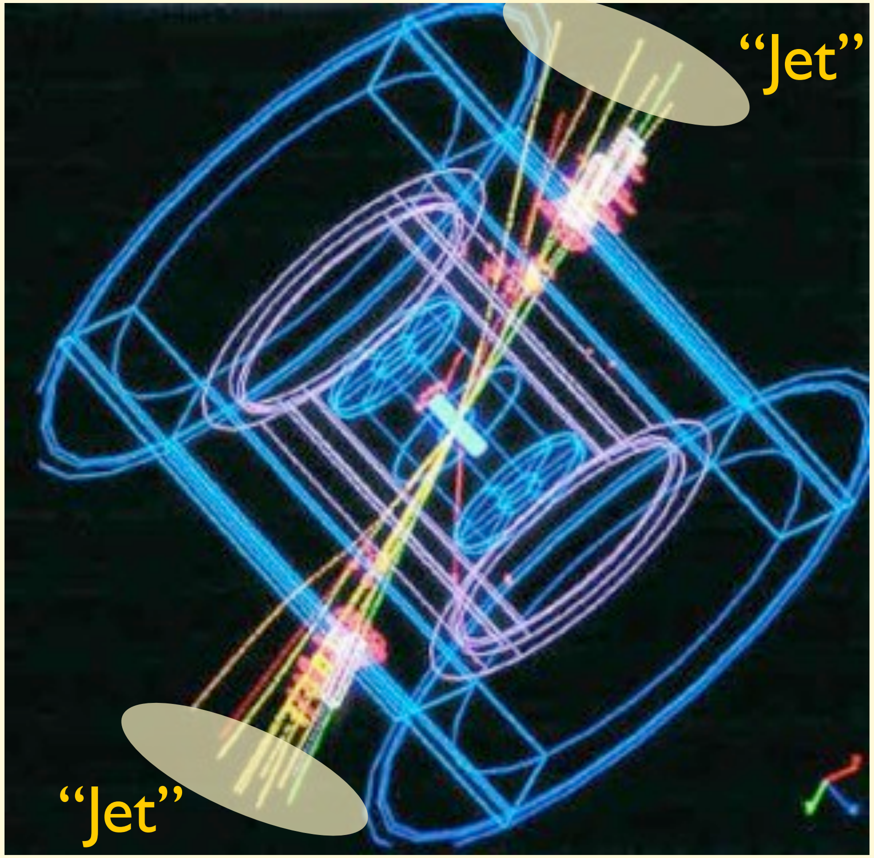

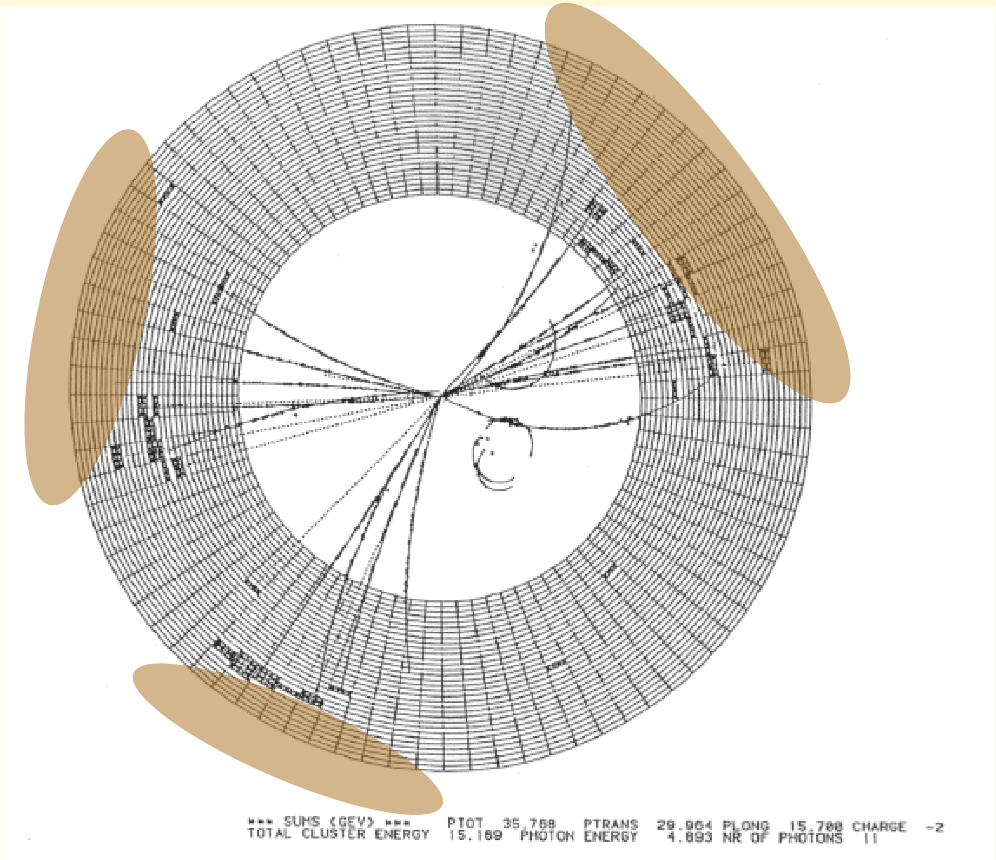

$e^+ e^- \to qq$ ⇨ $e^+ e^- \to$ 2 jets

$e^+ e^- \to qqg$ ⇨ $e^+ e^- \to$ 3 jets

The puzzle appears to be solved by associating partons to collimated "**jets**" of hadrons

Soft gluon emission

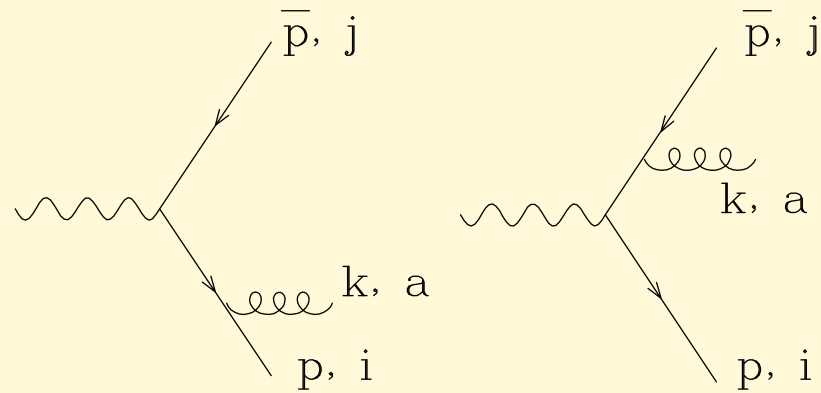

$$
\begin{aligned}
A &= \bar{u}(p)\epsilon(k)(ig)\,\frac{-i}{\not p + \not k}\,\Gamma^\mu\, v(\bar p)\ \lambda^a_{ij} + \bar{u}(p)\,\Gamma^\mu\,\frac{i}{\not{\bar p} + \not k}\,(ig)\epsilon(k)\,v(\bar p)\ \lambda^a_{ij} \\
&= \left[\frac{g}{2p\cdot k}\bar{u}(p)\epsilon(k)\,(\not p + \not k)\Gamma^\mu\, v(\bar p) - \frac{g}{2\bar p\cdot k}\bar{u}(p)\,\Gamma^\mu\,(\not{\bar p} + \not k)\epsilon(k)\,v(\bar p)\right]\lambda^a_{ij}
\end{aligned}
$$

$p\cdot k = p_0\, k_0\, (1-\cos\theta) \Rightarrow$ singularities for collinear ($\cos\theta \to 1$) or soft ($k_0 \to 0$) emission

Collinear emission does not alter the global structure of the final state, since its preserves its "pencil-like-ness". **Soft emission** at large angle, however, could spoil the structure, and leads to strong interferences between emissions from different legs. So soft emission needs to be studied in more detail.

In the soft ($k_0 \to 0$) limit the amplitude simplifies and ***factorizes*** as follows:

Exercise:

$$A_{soft} = g\lambda^a_{ij}\left(\frac{p\cdot\epsilon}{p\cdot k} - \frac{\bar p\cdot\epsilon}{\bar p\cdot k}\right) A_{Born}$$

Factorization: it is the expression of the independence of long-wavelength (soft) emission on the nature of the hard (short-distance) process.

Another simple derivation of soft-gluon emission rules

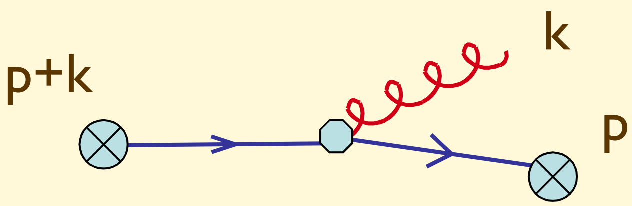

charge current of a free fermion

$$\bar{\psi}(p)\,\gamma_\mu\,\psi(p+k)\,\epsilon^\mu(k) \quad \stackrel{k\to 0}{\longrightarrow} \quad \bar{\psi}(p)\,\gamma_\mu\,\psi(p)\epsilon^\mu(k) \;=\; 2p\cdot\epsilon$$

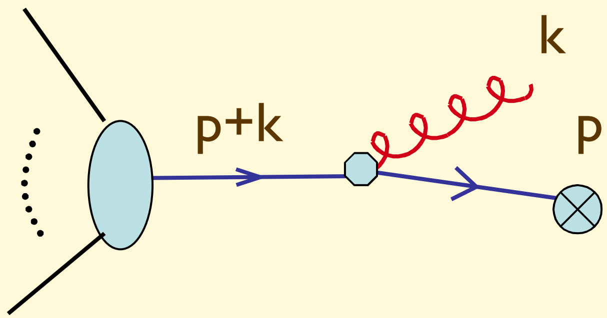

$$\frac{1}{\not p + \not k}\gamma_\mu \psi(p)\,\varepsilon^\mu(k) \quad \stackrel{k\to 0}{\longrightarrow}$$

$$\frac{1}{2p\cdot k}\not p \gamma_\mu \psi(p)\varepsilon^\mu(k) \;=\; \frac{p\cdot\varepsilon}{p\cdot k}\psi(p)$$

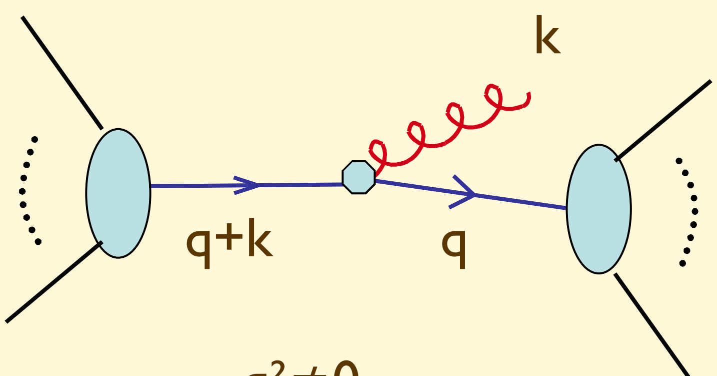

$q^2 \neq 0$

$$\frac{1}{\not q + \not k}\gamma_\mu \frac{1}{\not q}\,\varepsilon^\mu(k) \quad \stackrel{q^2\neq 0,\, k\to 0}{\longrightarrow} \quad \frac{1}{q^2}\not q \gamma_\mu \not q \frac{1}{q^2}\varepsilon^\mu(k)$$

=> finite

Similar, but more structured, result in the case of a fully coloured process:

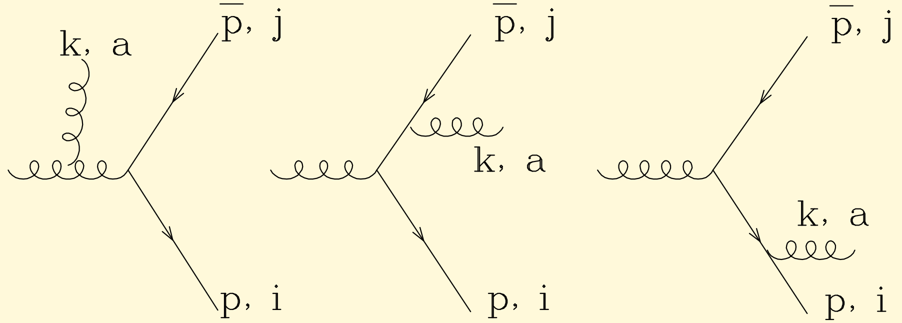

$$A_{soft} = g\,(\lambda^a \lambda^b)_{ij} \left[\frac{Q\varepsilon}{Qk} - \frac{\bar{p}\varepsilon}{\bar{p}k} \right] + g\,(\lambda^b \lambda^a)_{ij} \left[\frac{p\varepsilon}{pk} - \frac{Q\varepsilon}{Qk} \right]$$

The four terms correspond to the two possible ways colour can flow, and to the two possible emissions for each colour flow:

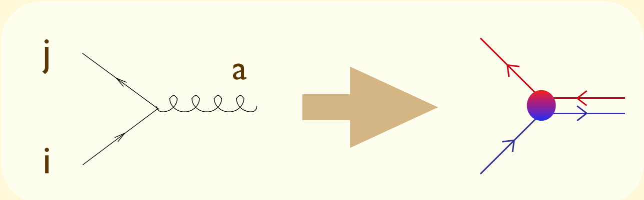

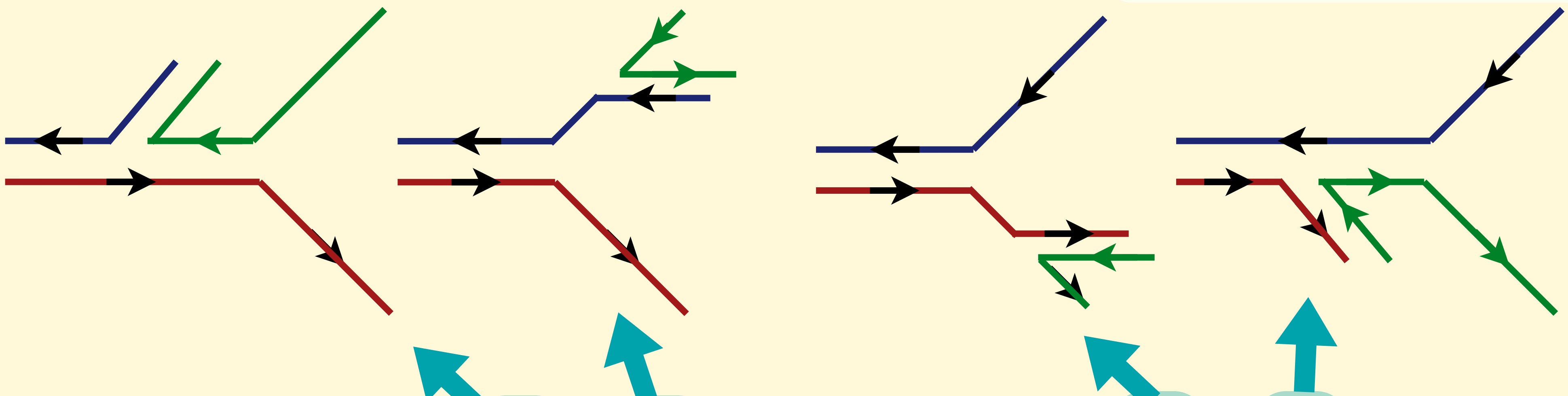

$$A_{soft} = g\,(\lambda^a \lambda^b)_{ij} \left[\frac{Q\varepsilon}{Qk} - \frac{\bar{p}\varepsilon}{\bar{p}k} \right] + g\,(\lambda^b \lambda^a)_{ij} \left[\frac{p\varepsilon}{pk} - \frac{Q\varepsilon}{Qk} \right]$$

The interference between the two colour structures

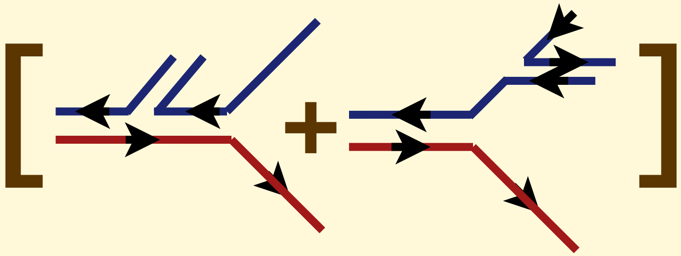 $\propto (\lambda^a \lambda^b)_{ij}$ 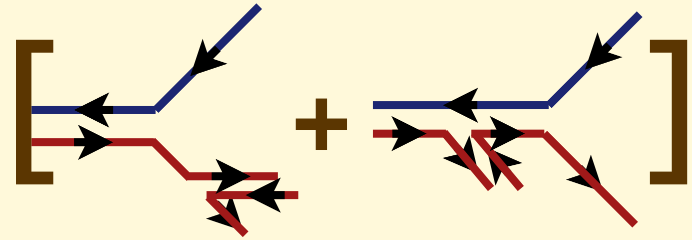 $\propto (\lambda^b \lambda^a)_{ij}$

is suppressed by $1/N_c^2$:

$$\sum_{a,b,i,j} |(\lambda^a\lambda^b)_{ij}|^2 = \sum_{a,b} tr\ \left(\lambda^a\lambda^b\lambda^b\lambda^a\right) = \frac{N^2-1}{2} C_F = O(N^3)$$

$$\sum_{a,b,i,j} (\lambda^a\lambda^b)_{ij}[(\lambda^b\lambda^a)_{ij}]^* = \sum_{a,b} tr(\lambda^a\lambda^b\lambda^a\lambda^b) = \frac{N^2-1}{2} \underbrace{(C_F - \frac{C_A}{2})}_{-\frac{1}{2N}} = O(N)$$

As a result, the emission of a soft gluon can be described, to the leading order in $1/N_c^2$, as the incoherent sum of the emission from the two colour currents

What about the interference between the two diagrams corresponding to the same colour flow? ➥

Angular ordering

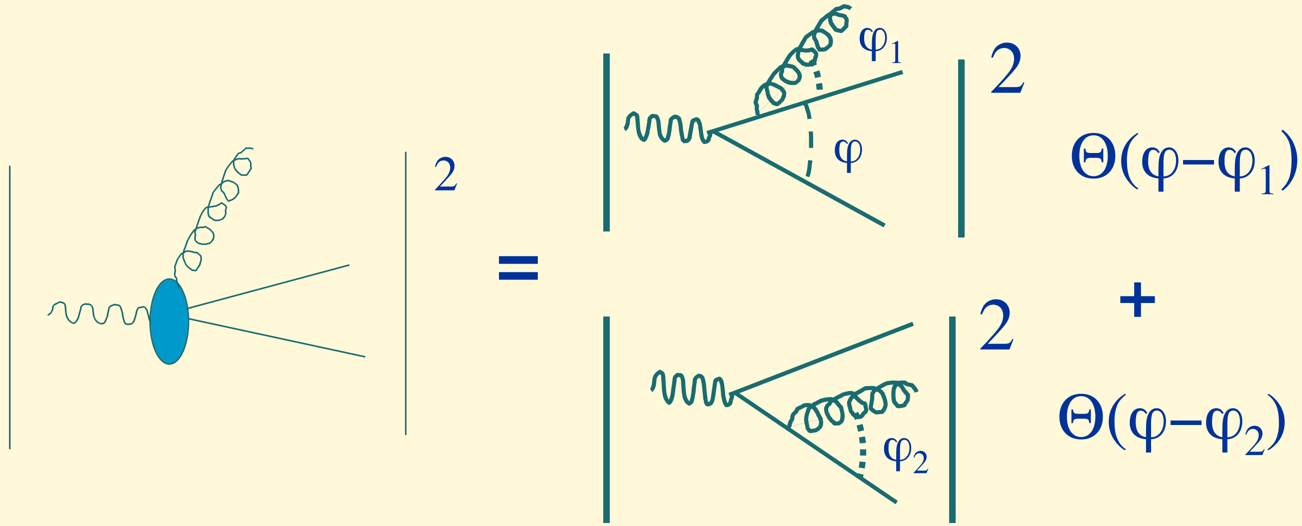

Radiation inside the cones is allowed, and described by the eikonal probability, radiation outside the cones is suppressed and averages to 0 when integrated over the full azimuth

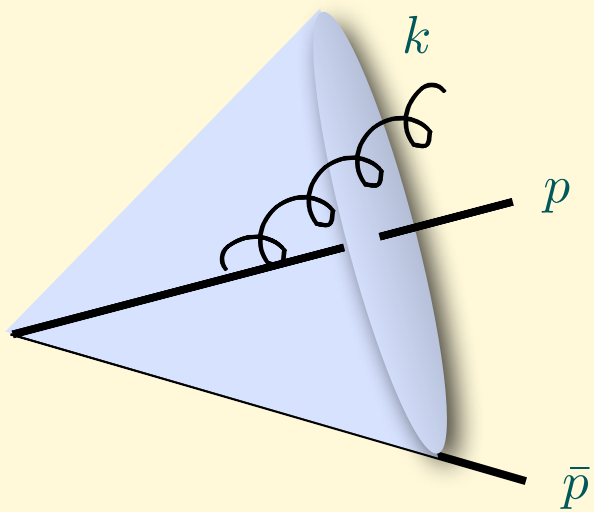

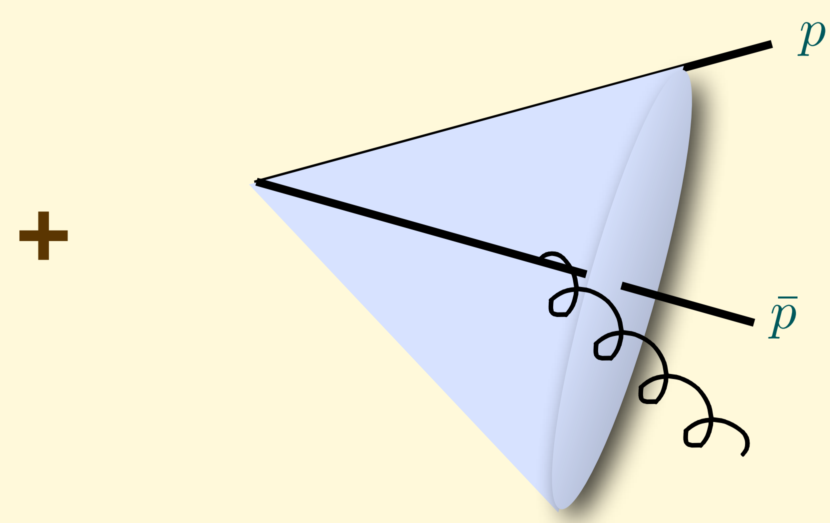

$$\frac{p\cdot\bar{p}}{(p\cdot k)(\bar{p}\cdot k)}\left[\Theta(\phi-\phi_1)+\Theta(\phi-\phi_2)\right]$$

An intuitive explanation of angular ordering

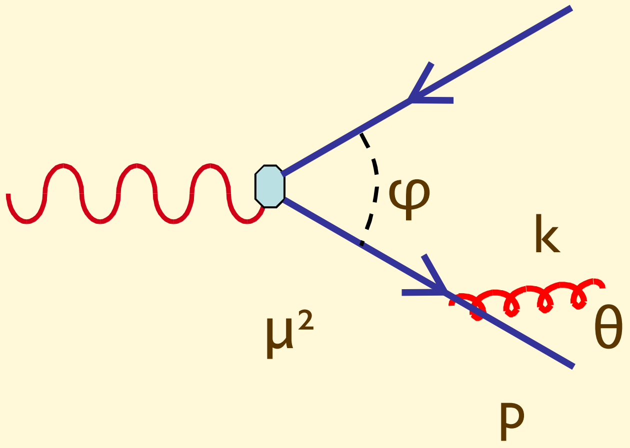

Lifetime of the virtual intermediate state:

$$\tau < \gamma/\mu = E/\mu^2 = 1 / (k_0\theta^2) = 1/(k_\perp\theta)$$

$$\mu^2 = (p+k)^2 = 2E\, k_0\, (1-\cos\theta)$$
$$\sim E\, k_0\, \theta^2 \sim E\, k_\perp\, \theta$$

Distance between q and qbar after τ:

$$d = \varphi\tau = (\varphi/\theta)\ 1/k_\perp$$

If the transverse wavelength of the emitted gluon is longer than the separation between q and qbar, the gluon emission is suppressed, because the q qbar system will appear as colour neutral (=> dipole-like emission, suppressed)

Therefore $d > 1/k_\perp$, which implies $\theta < \varphi$

The formal proof of angular ordering

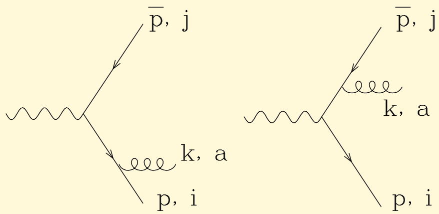

$$d\sigma_g = \sum |A_{soft}|^2 \frac{d^3k}{(2\pi)^3 2k^0} \sum |A_0|^2 \frac{-2p^\mu p^\nu}{(pk)(pk)} g^2 \sum \varepsilon_\mu \varepsilon^*_\nu \frac{d^3k}{(2\pi)^3 2k^0}$$

$$= d\sigma_0 \frac{\alpha_s C_F}{\pi} \frac{dk^0}{k^0} \frac{d\phi}{2\pi} \frac{1-\cos\theta_{ij}}{(1-\cos\theta_{ik})(1-\cos\theta_{jk})} d\cos\theta$$

You can easily prove that:

$$\frac{1-\cos\theta_{ij}}{(1-\cos\theta_{ik})(1-\cos\theta_{jk})} = \frac{1}{2}\left[\frac{\cos\theta_{jk}-\cos\theta_{ij}}{(1-\cos\theta_{ik})(1-\cos\theta_{jk})} + \frac{1}{1-\cos\theta_{ik}}\right] + \frac{1}{2}[i \leftrightarrow j] \equiv W_{(i)} + W_{(j)}$$

where:

$$W_{(i)} \rightarrow finite\ if\ k \parallel j\ (\cos\theta_{jk} \rightarrow 1)$$
$$W_{(j)} \rightarrow finite\ if\ k \parallel i\ (\cos\theta_{ik} \rightarrow 1)$$

The probabilistic interpretation of W(i) and W(j) is a priori spoiled by their non-positivity. However, you can prove that after azimuthal averaging:

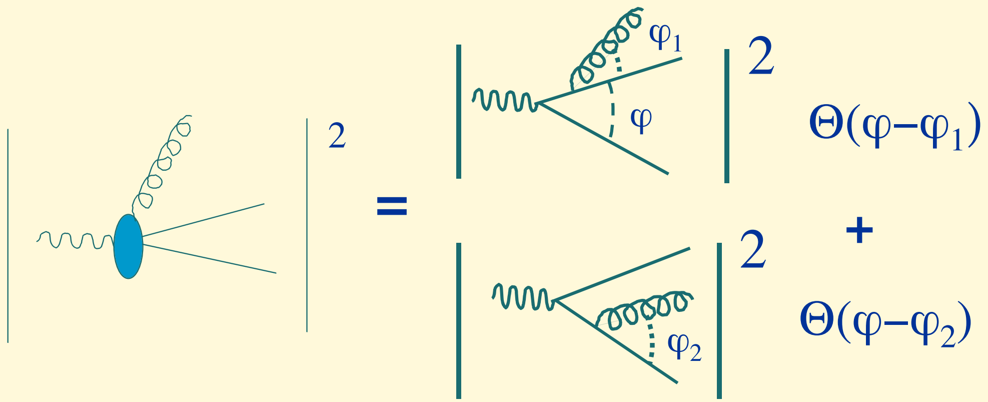

$$\int \frac{d\phi}{2\pi} W_{(i)} = \frac{1}{1-\cos\theta_{ik}} \text{ if } \theta_{ik} < \theta_{ij}\,, \quad 0 \text{ otherwise}$$

$$\int \frac{d\phi}{2\pi} W_{(j)} = \frac{1}{1-\cos\theta_{jk}} \text{ if } \theta_{jk} < \theta_{ij}\,, \quad 0 \text{ otherwise}$$

Further branchings will obey angular ordering relative to the new angles. As a result emission angles get smaller and smaller, squeezing the jet

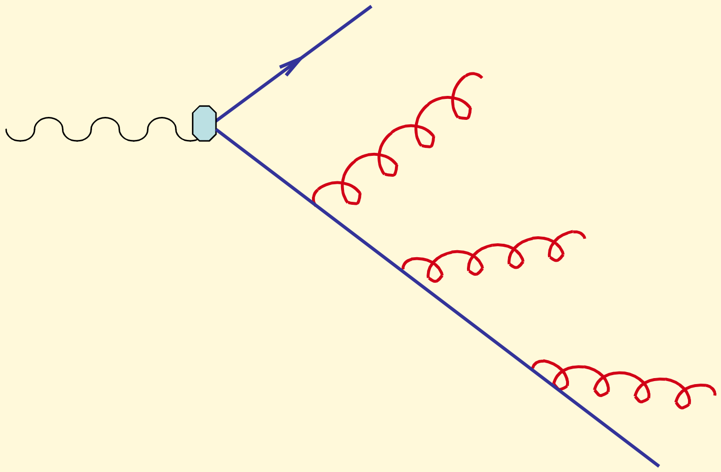

The construction can be iterated to the next emission, with the result that emission angles keep getting smaller and smaller => **jet structure**

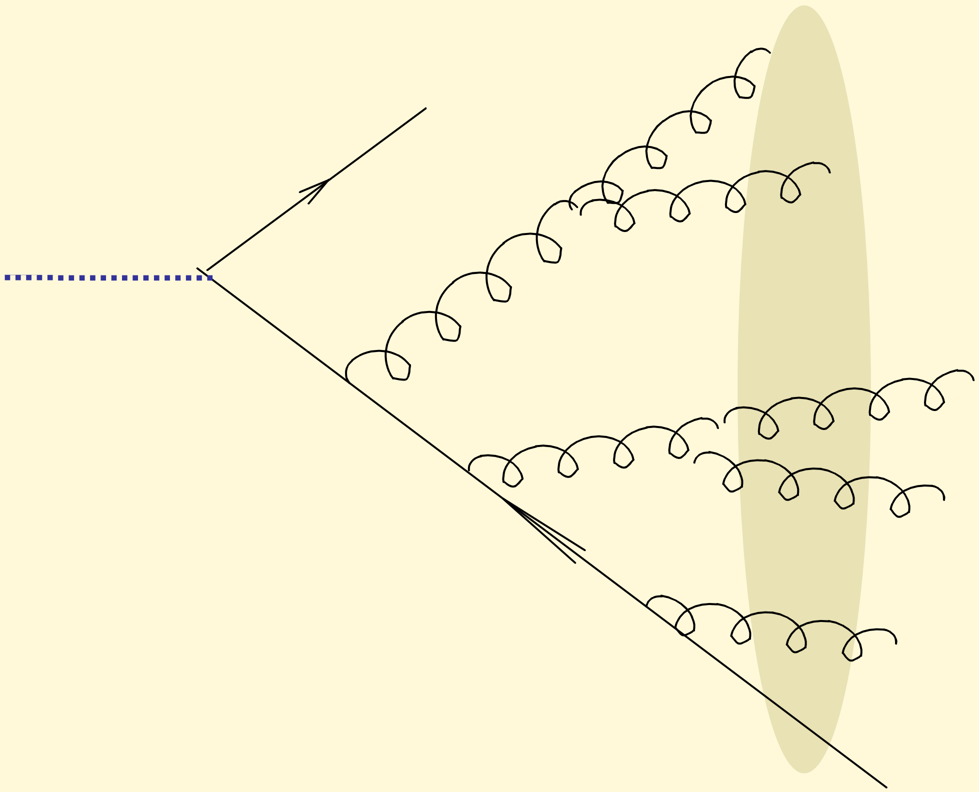

Total colour charge of the system is equal to the quark colour charge. Treating the system as the incoherent superposition of N gluons would lead to artificial growth of gluon multiplicity. Angular ordering enforces coherence, and leads to the proper evolution with energy of particle multiplicities.

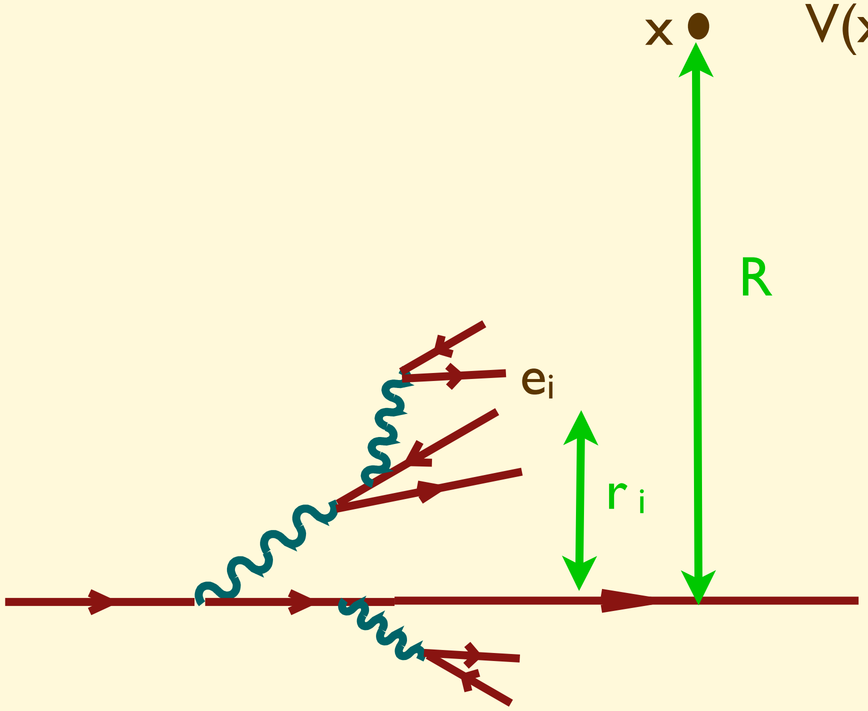

$$V(x) = \frac{e}{R} + \frac{1}{R^2} \left| \sum e_i \boldsymbol{r}_i \right|$$

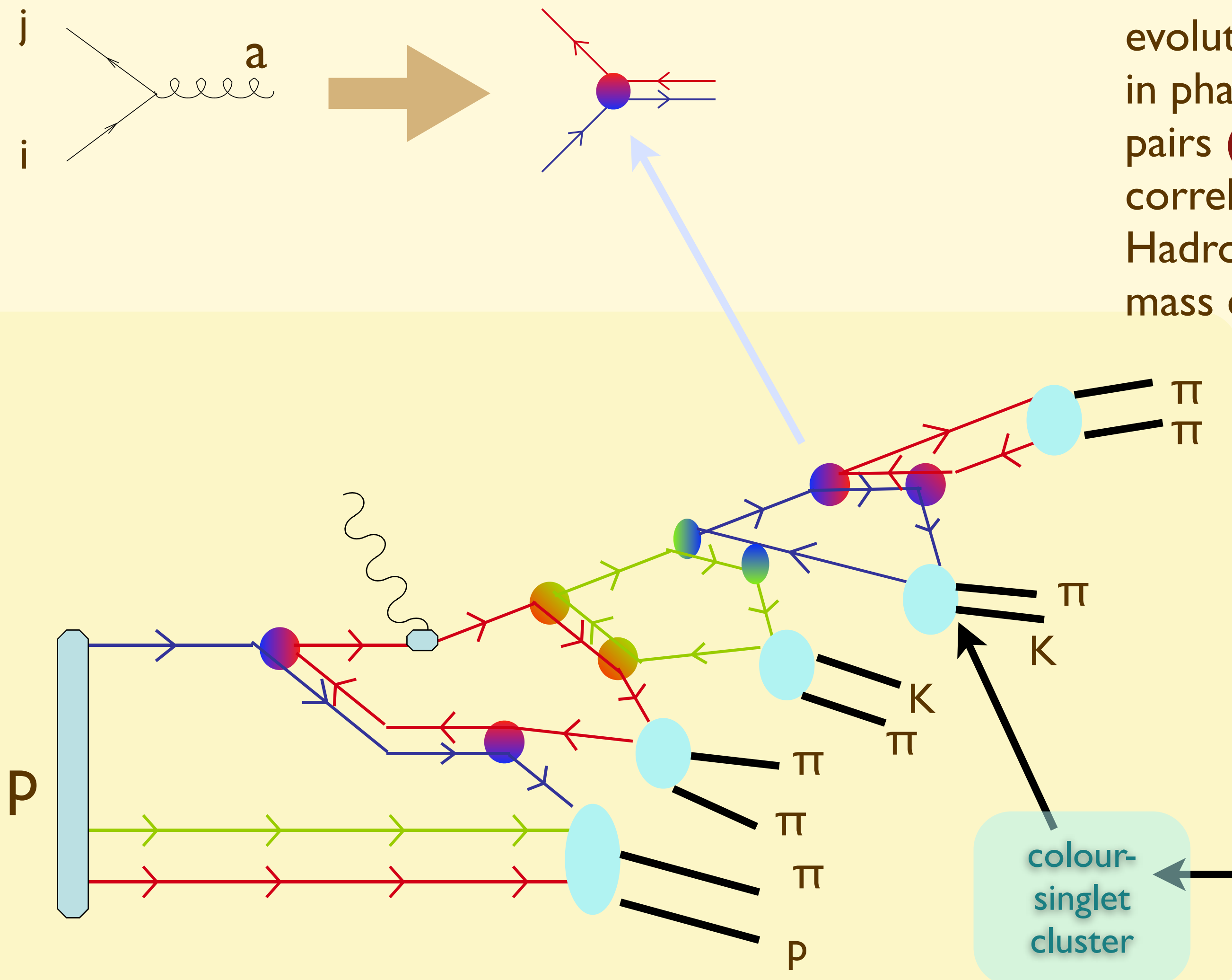

The structure of the perturbative evolution leads naturally to the clustering in phase-space of colour-singlet parton pairs ("preconfinement"). Long-range correlations are strongly suppressed. Hadronization will only act locally, on low-mass colour-singlet clusters.

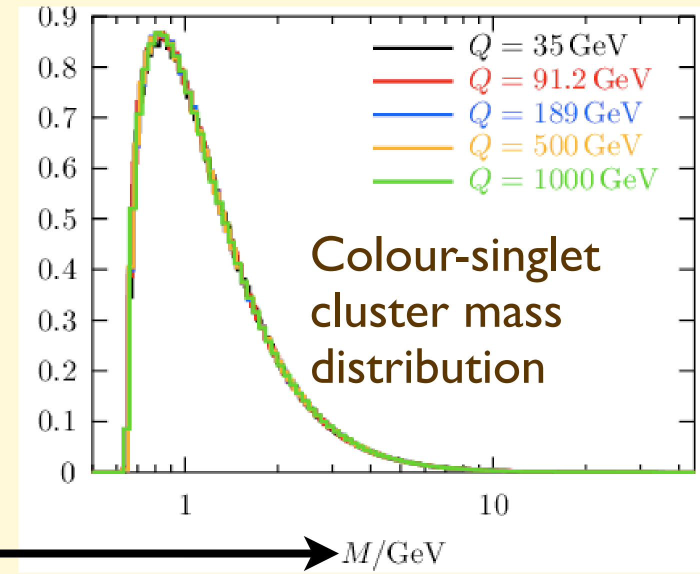

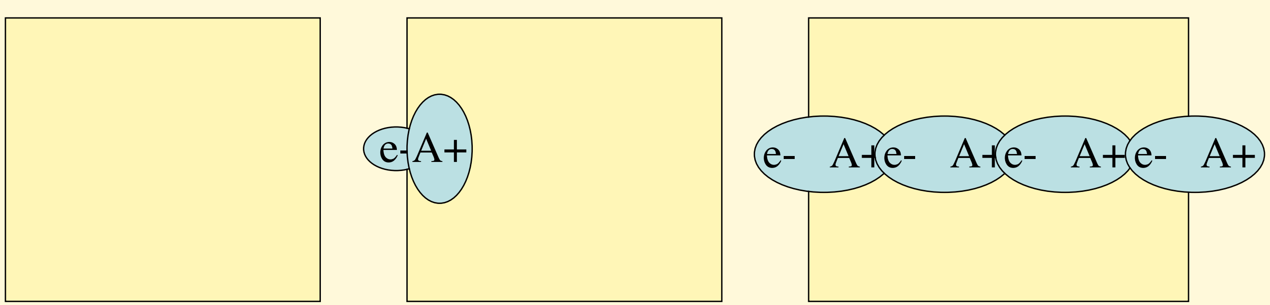

Colour is left "behind" by the struck quark. The first soft gluon emitted at large angle will connect to the beam fragments, ensuring that the beam fragments can recombine to form hadrons, and will allow the struck quark to evolve without having to worry about what happens to the proton fragments.

Shower Monte Carlos

Goal: complete description of the event, at the level of individual hadrons

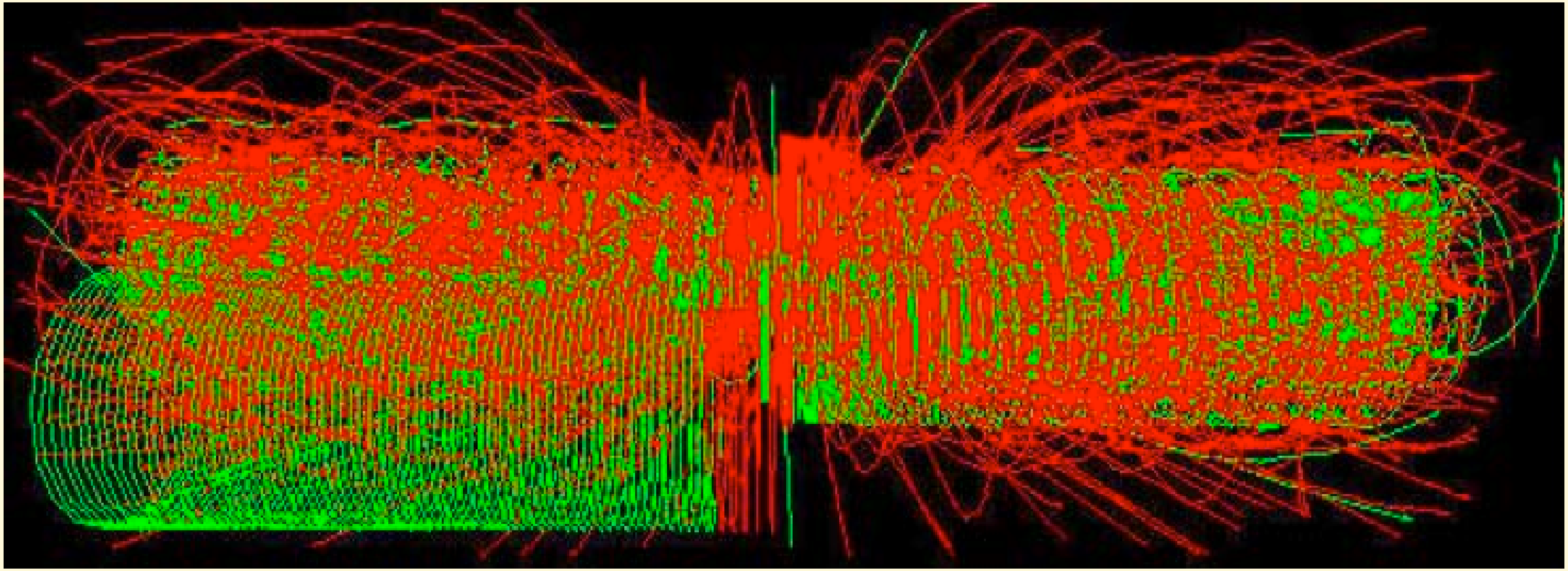

I: Generate the parton-level hard event

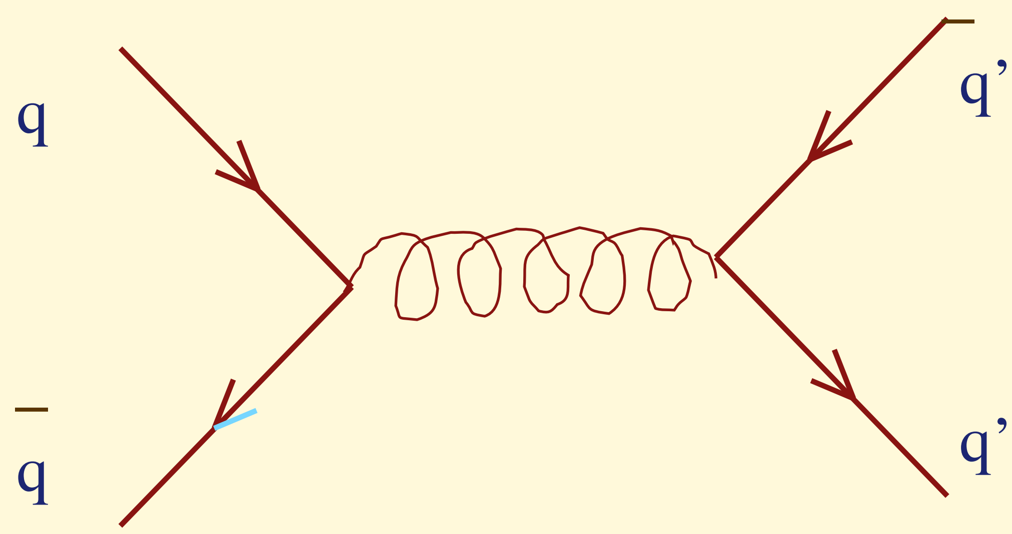

II: Develop the parton shower

1. Final state

2. Initial state

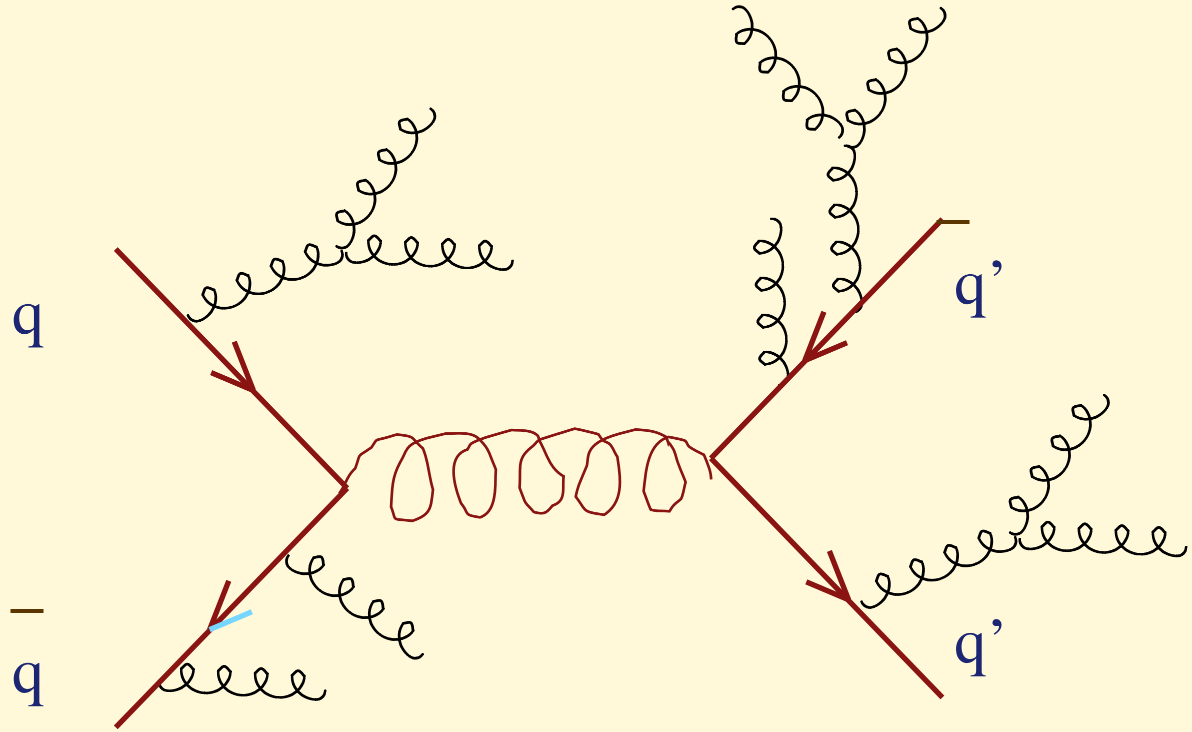

III: Hadronize partons

1. Split gluons into q-qbar pairs
2. Connect colour-singlet pairs
3. Decay the colour-singlet clusters into hadron pairs

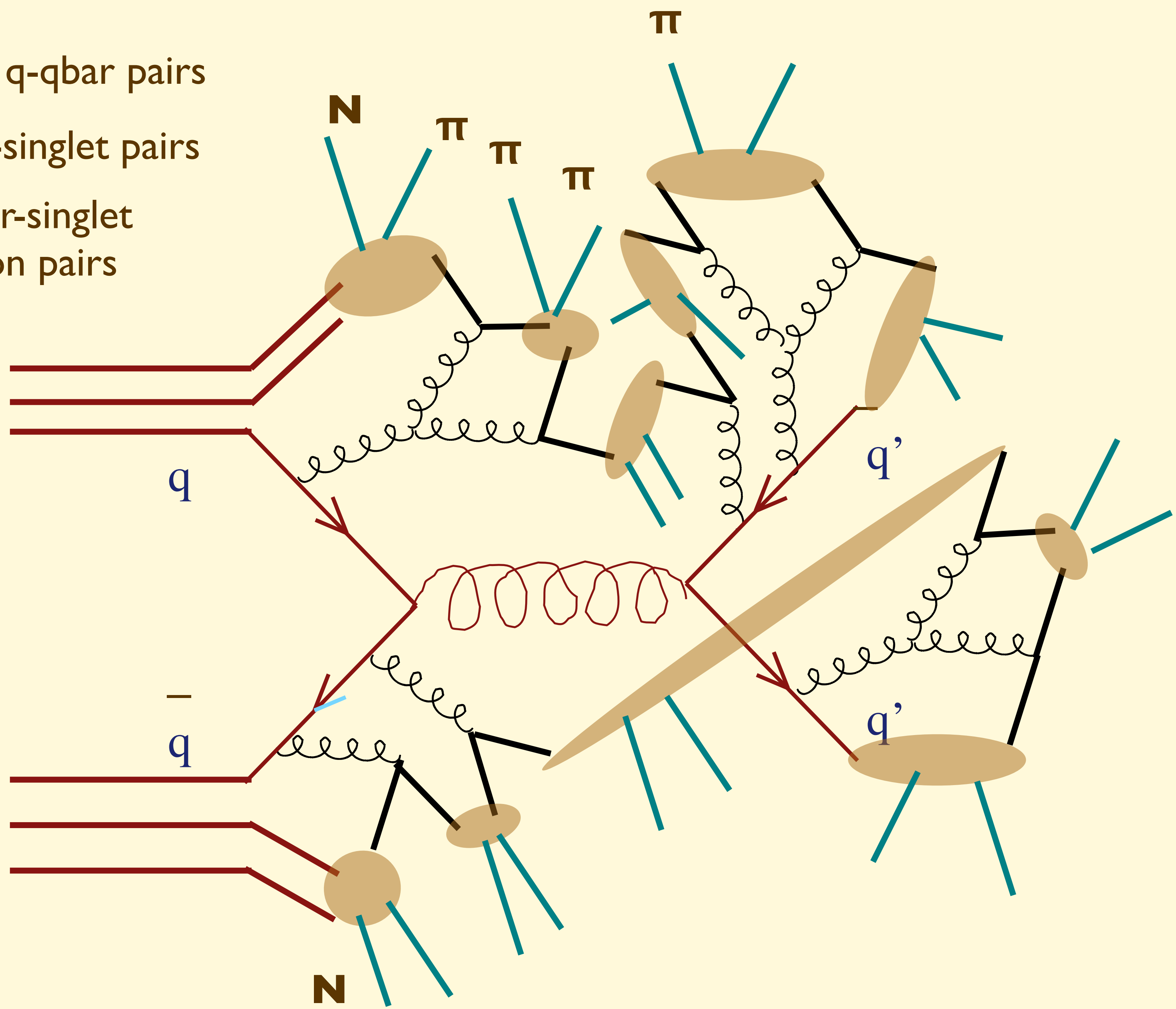

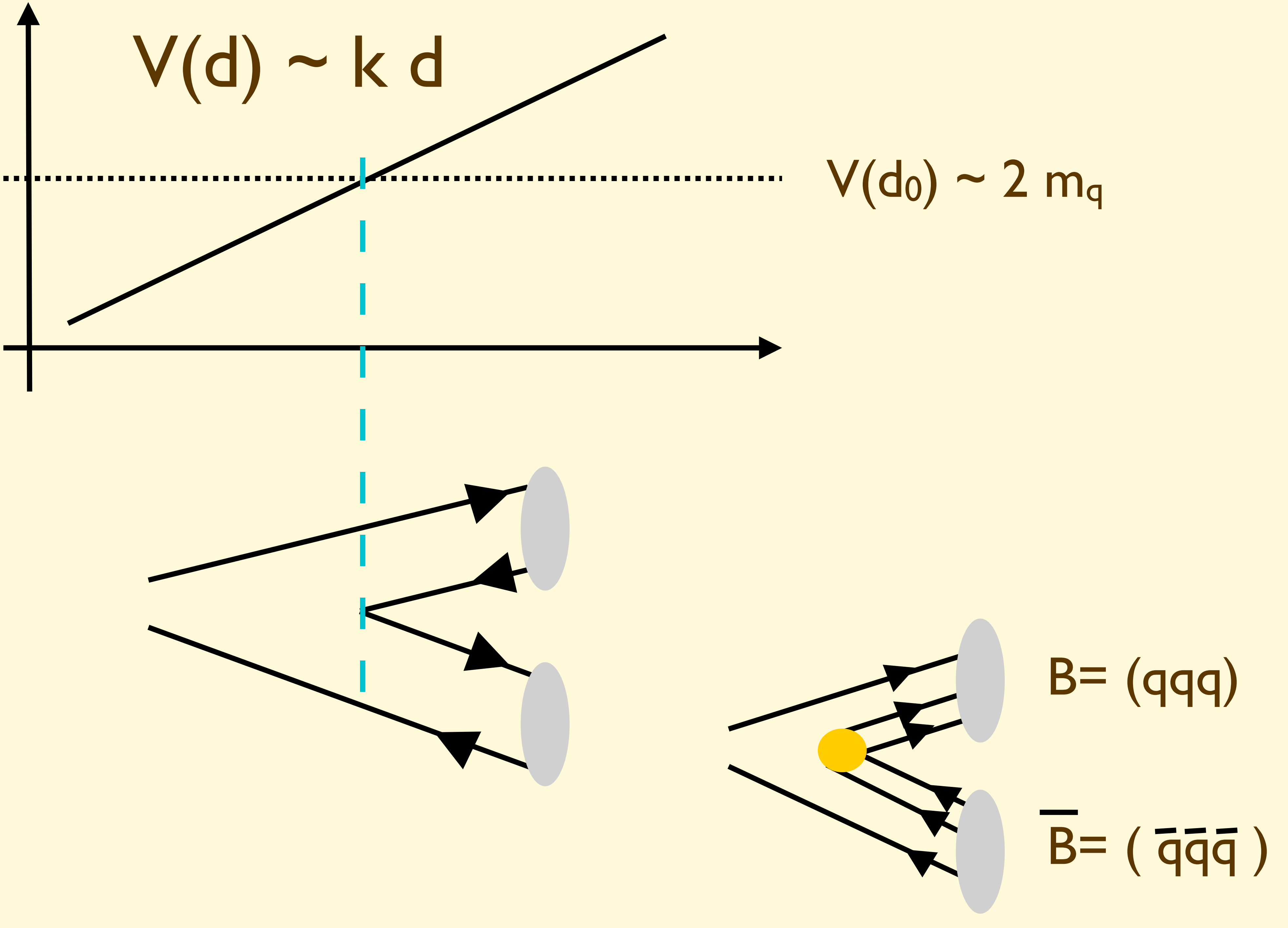
V(d) ~ k d
V(d0) ~ 2 mq
B= (qqq)
B= (q̄q̄q̄)

The shower algorithm

Sequential probabilistic evolution (Markov chain)

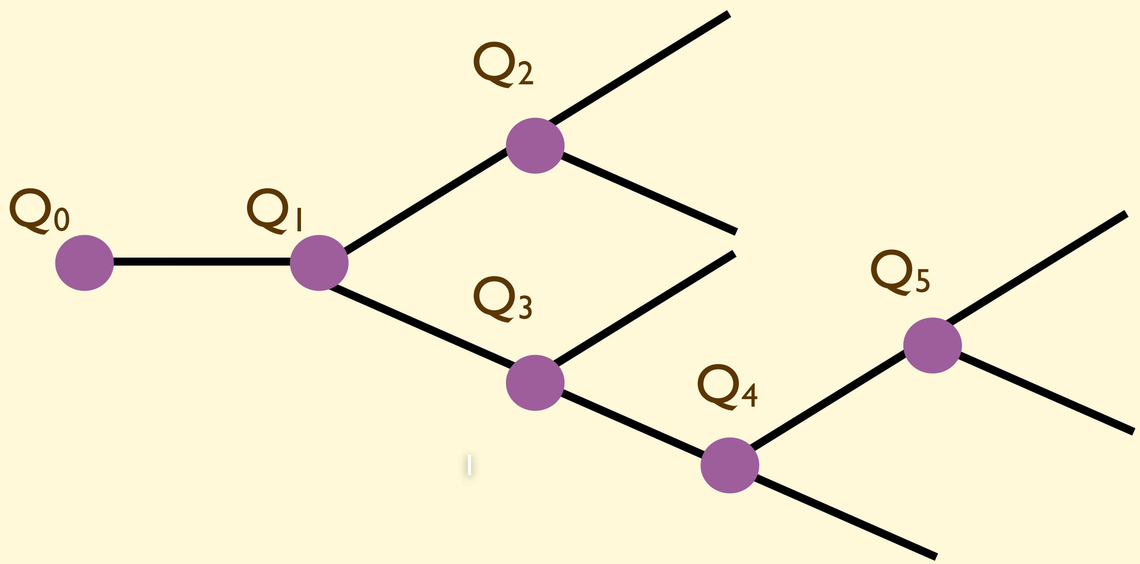

The probability of each emission only depends on the state of the splitting parton, and of the daughters. The QCD dynamics is encoded in these splitting probabilities.

The total probability of all possible evolutions is 1 (unitary evolution).

- The shower evolution does not change the event rate inherited from the parton level, matrix element computation.
- No K-factors from the shower, even though the shower describes higher-order corrections to the leading-order process

Single emission

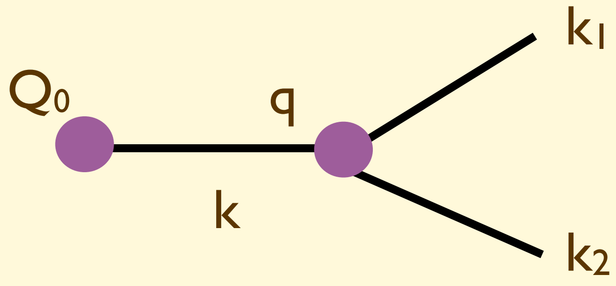

$$\frac{d\mathrm{Prob}(Q_0 \to q^2)}{dq^2\, dz\, d\phi} = P_0 \frac{\alpha_s(\mu)}{2\pi} \frac{1}{q^2} P(z)$$

$P_0 \Rightarrow \int d\,\mathrm{Prob} = 1$

q^2 $\approx$ virtuality scale of the branching:

- **$(k_1 + k_2)^2$**
- **$k_1 \cdot k_2$**
- **$k_\perp{}^2$**
- **....**

ϕ = azimuth

$z=P(k_2)/P(k)$ $\approx$ energy/momentum fraction carried by one of the two partons after splitting

- **$P=k^0$**
- **$P=k_{//}$**
- **$P=k_{//} + k^0$**
- **...**

$\mu = f(z,q)$

While at leading-logarithmic order (LL) all choices of evolution variables and of scale for α_s are equivalent, specific choices can lead to improved description of NLL effects and allow a more accurate and easy-to-implement inclusion of angular-ordering constraints and mass effects, as well as to a better merging of multijet ME's with the shower

Multiple emission

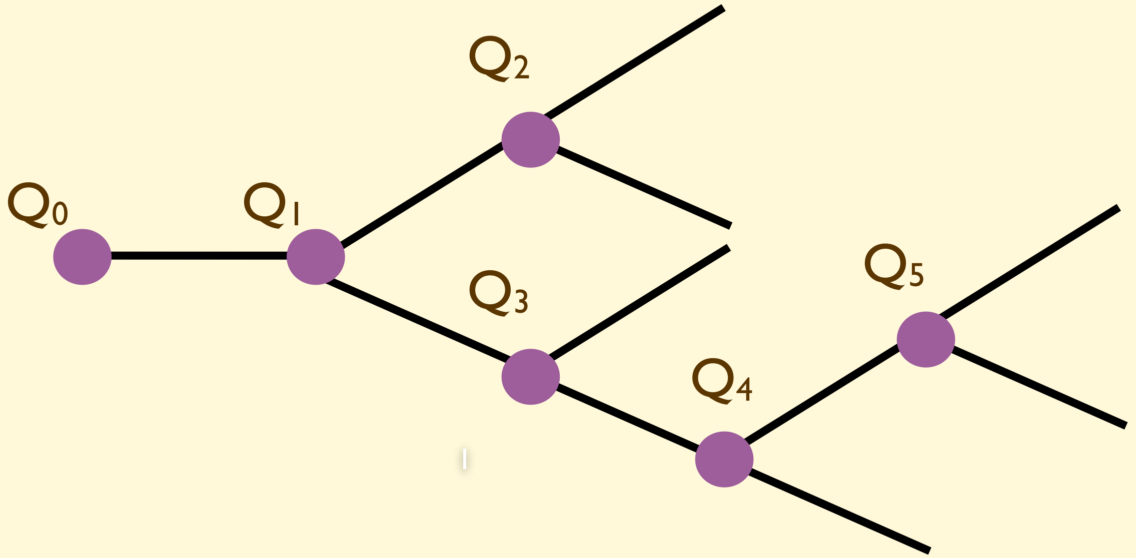

$$\mathrm{Prob}(Q_0 \to Q_1) = P_0 \frac{\alpha_s}{2\pi} \int_{Q_1}^{Q_0} \frac{dq^2}{q^2} dz P(z) d\phi$$

$$\mathrm{Prob}(Q_0 \to Q_1 \to Q_2) = P_0 \frac{\alpha_s}{2\pi} \int_{Q_1}^{Q_0} \frac{dq^2}{q^2} dz P(z) d\phi \frac{\alpha_s}{2\pi} \int_{Q_2}^{Q_1} \frac{dq^2}{q^2} dz P(z) d\phi$$

$$\sim P_0 \frac{1}{2!} [\frac{\alpha_s}{2\pi} \int_{Q_2}^{Q_0} \frac{dq^2}{q^2} dz P(z) d\phi]^2$$

$$\mathrm{Prob}(Q_0 \to X) = P_0 \times \sum \frac{1}{n!} [\frac{\alpha_s}{2\pi} \int_{\Lambda}^{Q_0} \frac{dq^2}{q^2} dz P(z) d\phi]^n = 1$$

Λ=infrared cutoff

$$P_0 = \exp\{-\frac{\alpha_s}{2\pi} \int_{\Lambda}^{Q_0} \frac{dq^2}{q^2} dz P(z) d\phi\}$$

P_0 = Sudakov form factor
~ probability of no emission between the scale Q_0 and Λ

Generation of splittings

$$P(Q,\Lambda) = exp\left[-\int_{\Lambda}^{Q}\frac{dq^2}{q^2}\frac{\alpha_s(q)}{2\pi}P(z)dz\right]$$

prob. of no radiation between Q and Λ

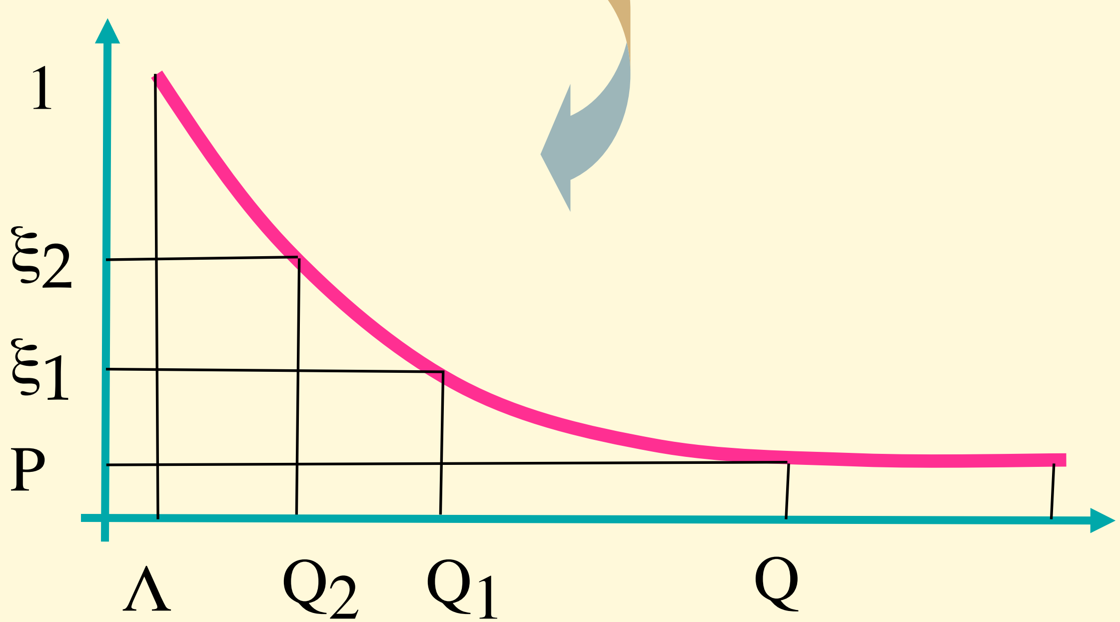

1. Generate $0< \xi_1 <1$
2. If ξ_1 < P(Q , Λ) ⇒ no radiation, q' goes directly on-shell at scale Λ≈GeV
3. Else
    1. calculate Q_1 such that $P(Q_1,\Lambda)= \xi_1$
    2. emission at scale Q_1:

4. Select z according to P(z)
5. Reconstruct the full kinematics of the splitting
6. Go back to 1) and reiterate, until shower stops in 2). At each step the probability of emission gets smaller and smaller

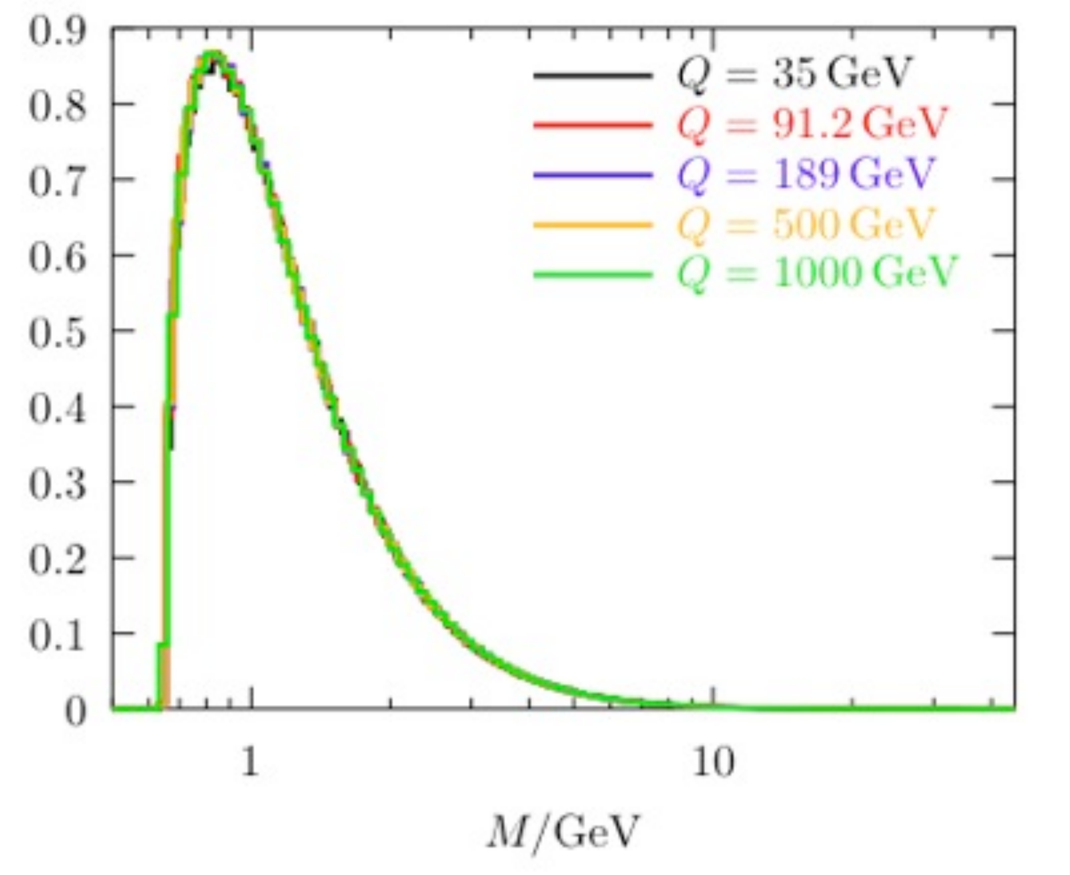

The existence of high-mass clusters, however rare, is unavoidable, due to IR cutoff which leads to a non-zero probability that no emission takes place. This is particularly true for evolution of massive quarks (as in, e.g. Z→bb or cc). Prescriptions have to be defined to deal with the "evolution" of these clusters. **This has an impact on the z→1 behaviour of fragmentation functions.**

Phenomenologically, this leads to uncertainties, for example, in the background rates for H→γγ (jet→γ).

This approach is extremely successful in describing the properties of hadronic final states!

Ex:
Particle multiplicities:

Particle	Experiment	Measured	Old model	Herwig (C^{++})	Herwig (Fortran)
All charged	M, A, D, L, O	20.924 ± 0.117	20.22*	20.814	20.532*
γ	A, O	21.27 ± 0.6	23.03	22.67	20.74
π^0	A, D, L, O	9.59 ± 0.33	10.27	10.08	9.88
$\rho(770)^0$	A, D	1.295 ± 0.125	1.235	1.316	1.07
$\pi^\pm$	A, O	17.04 ± 0.25	16.30	16.95	16.74
$\rho(770)^\pm$	O	2.4 ± 0.43	1.99	2.14	2.06
η	A, L, O	0.956 ± 0.049	0.886	0.893	0.669*
$\omega(782)$	A, L, O	1.083 ± 0.088	0.859	0.916	1.044
$\eta(958)$	A, L, O	0.152 ± 0.03	0.13	0.136	0.106
K^0	S, A, D, L, O	2.027 ± 0.025	2.121*	2.062	2.026
$K^*(892)^0$	A, D, O	0.761 ± 0.032	0.667	0.681	0.583*
$K^*(1430)^0$	D, O	0.106 ± 0.06	0.065	0.079	0.072
$K^\pm$	A, D, O	2.319 ± 0.079	2.335	2.286	2.250
$K^*(892)^\pm$	A, D, O	0.731 ± 0.058	0.637	0.657	0.578
$\phi(1020)$	A, D, O	0.097 ± 0.007	0.107	0.114	0.134*
p	A, D, O	0.991 ± 0.054	0.981	0.947	1.027
Δ^{++}	D, O	0.088 ± 0.034	0.185	0.092	0.209*
Σ^-	O	0.083 ± 0.011	0.063	0.071	0.071
Λ	A, D, L, O	0.373 ± 0.008	0.325*	0.384	0.347*
Σ^0	A, D, O	0.074 ± 0.009	0.078	0.091	0.063
Σ^+	O	0.099 ± 0.015	0.067	0.077	0.088
$\Sigma(1385)^\pm$	A, D, O	0.0471 ± 0.0046	0.057	0.0312*	0.061*
Ξ^-	A, D, O	0.0262 ± 0.001	0.024	0.0286	0.029
$\Xi(1530)^0$	A, D, O	0.0058 ± 0.001	0.026*	0.0288*	0.009*
Ω^-	A, D, O	0.00125 ± 0.00024	0.001	0.00144	0.0009*
$f_2(1270)$	D, L, O	0.168 ± 0.021	0.113	0.150	0.173
$f_2'(1525)$	D	0.02 ± 0.008	0.003	0.012	0.012
$D^\pm$	A, D, O	0.184 ± 0.018	0.322*	0.319*	0.283*
$D^*(2010)^\pm$	A, D, O	0.182 ± 0.009	0.168	0.180	0.151*
D^0	A, D, O	0.473 ± 0.026	0.625*	0.570*	0.501
$D_s^\pm$	A, O	0.129 ± 0.013	0.218*	0.195*	0.127
$D_s^{*\pm}$	O	0.096 ± 0.046	0.082	0.066	0.043
J/Ψ	A, D, L, O	0.00544 ± 0.00029	0.006	0.00361*	0.002*
Λ_c^+	D, O	0.077 ± 0.016	0.006*	0.023*	0.001*
$\Psi'(3685)$	D, L, O	0.00229 ± 0.00041	0.001*	0.00178	0.0008*

* Indicates a prediction that differs from the measured value by more than three standard deviations.

Tabl 1. Average particle multiplicities per event in e^+e^- collisions at 91.2 GeV. Experimental data were measured by the following collaborations at LEP and at SLC: ALEPH(A), DELPHI(D), L3(L), OPAL(O), MARK2(M), and SLD(S). The theoretical predictions in the last three columns, taken from Ref. [30], correspond to various implementations of the cluster hadronization model (see Ref. [30] for details).

30. Gieseke S et al. *JHEP* (02) 005 (2004)

Ex: Energy distributions

(Winter, Krauss, Soff,
hep-ph/0311085)

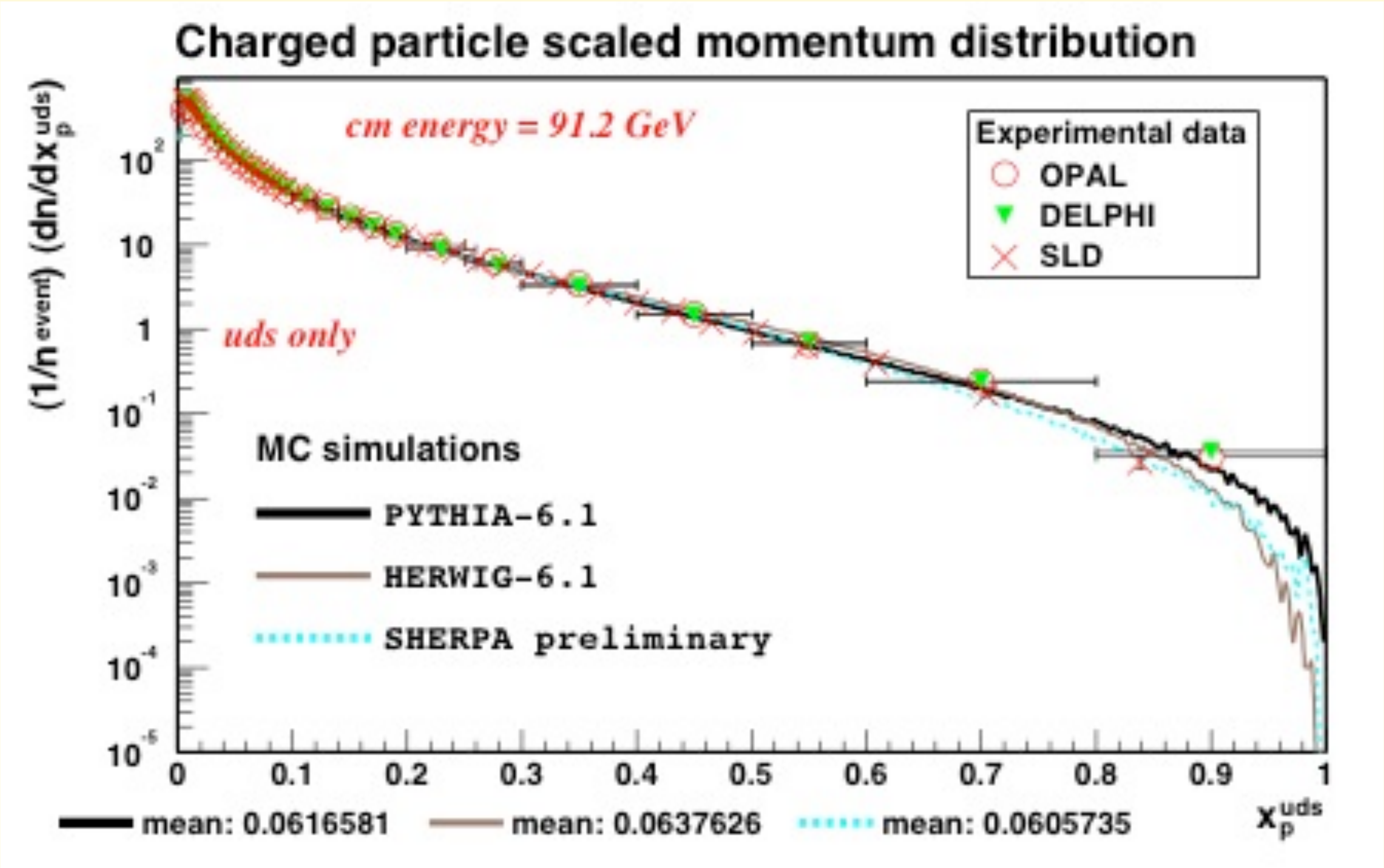

Ex: Transverse momenta w.r.t. thrust axis:

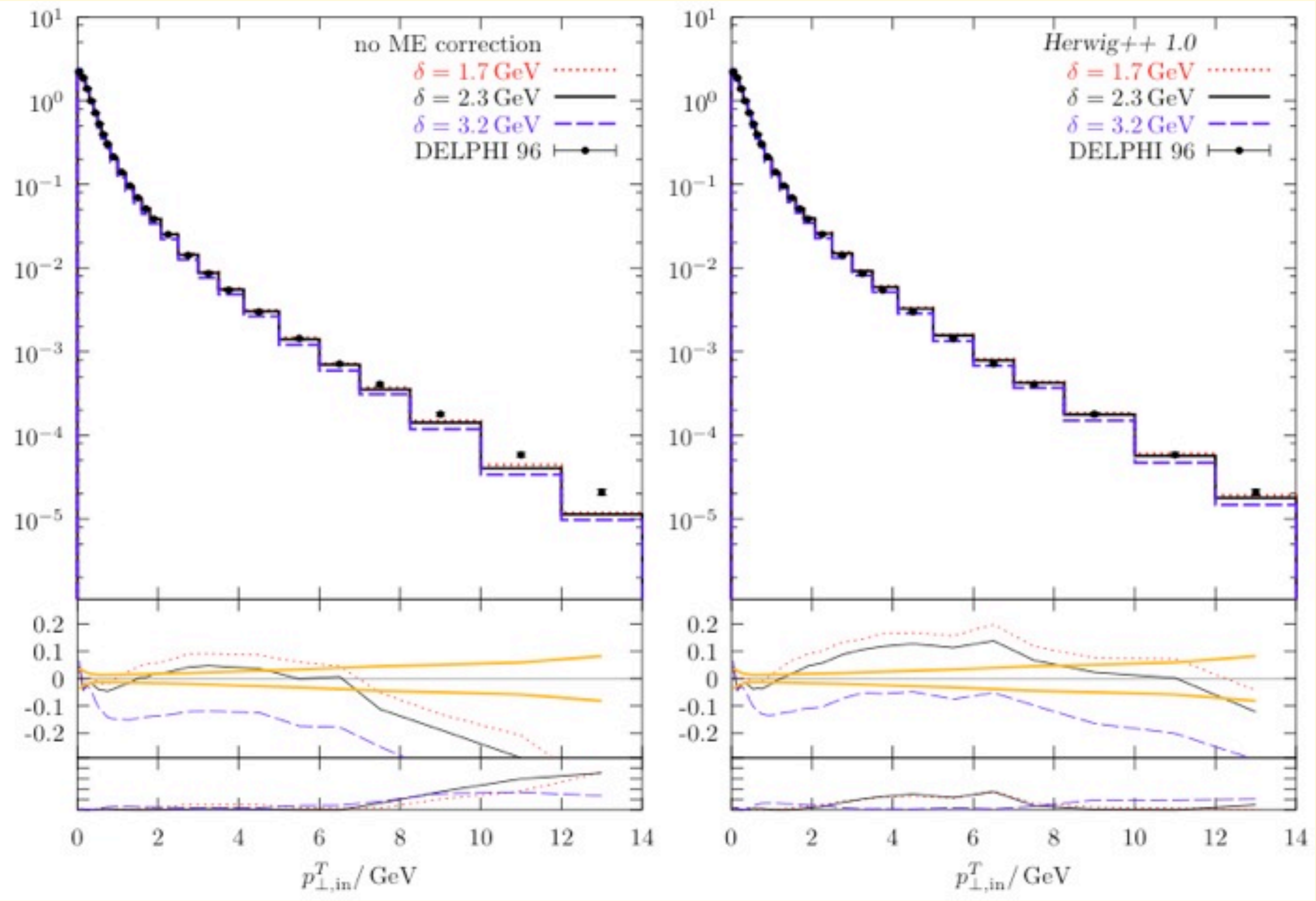

Jets in hadronic collisions

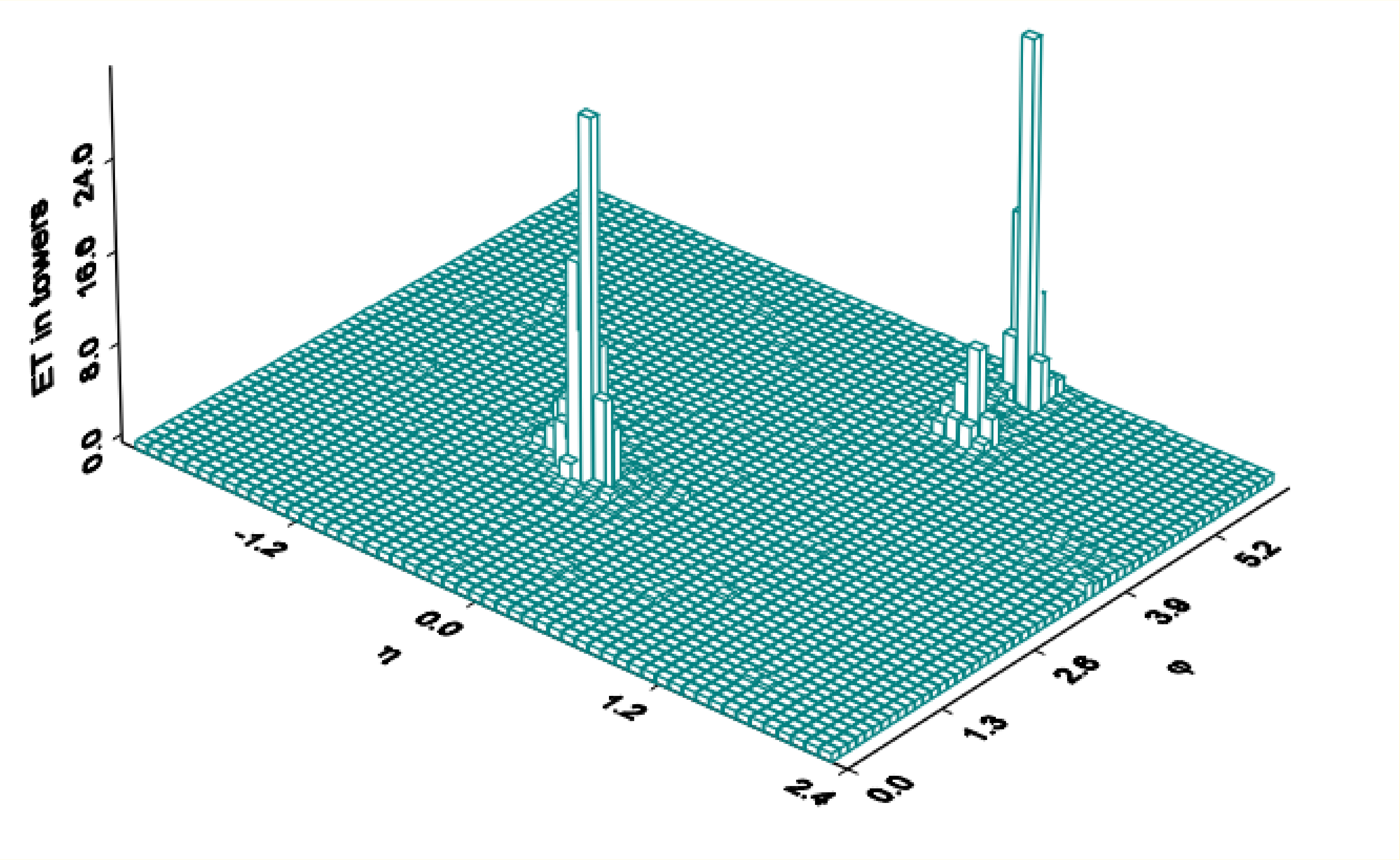

- Inclusive production of jets is the largest component of high-Q phenomena in hadronic collisions
- QCD predictions are known up to NLO accuracy
- Intrinsic theoretical uncertainty (at NLO) is approximately 10%
- Uncertainty due to knowledge of parton densities varies from 5-10% (at low transverse momentum, p_T to 100% (at very high p_T, corresponding to high-x gluons)
- Jet are used as probes of the quark structure (possible substructure implies departures from point-like behaviour of cross-section), or as probes of new particles (peaks in the invariant mass distribution of jet pairs)

$gg \to gg$

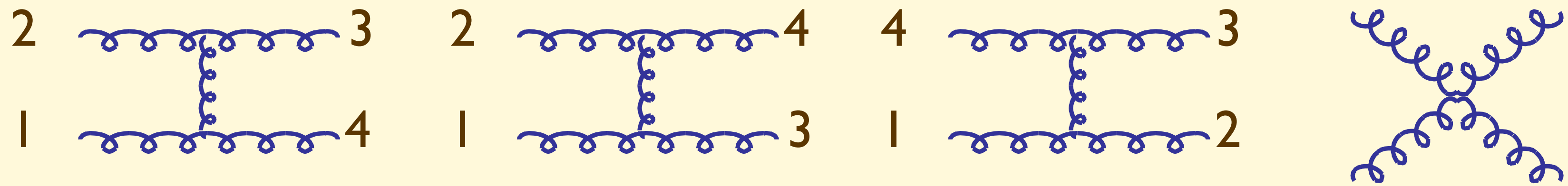

$gg \to q\bar{q}$

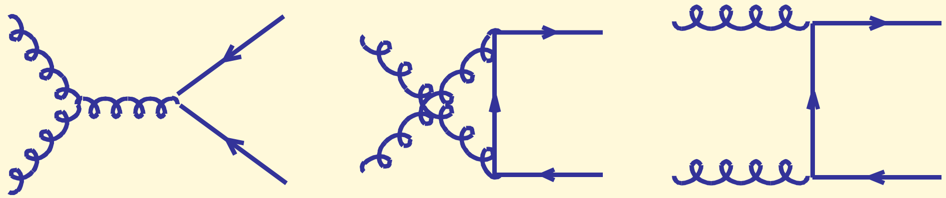

$qg \to qg$

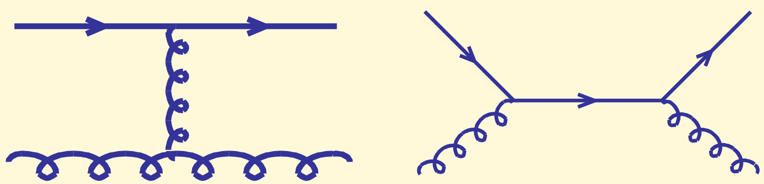

$q\bar{q} \to gg$

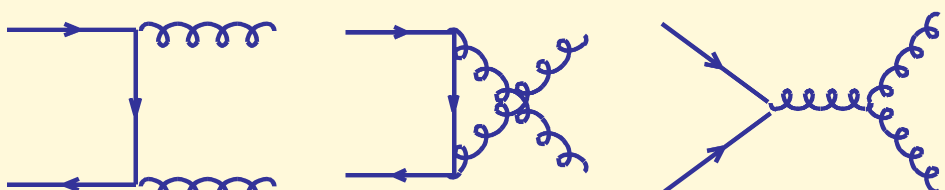

$qq' \to qq'$

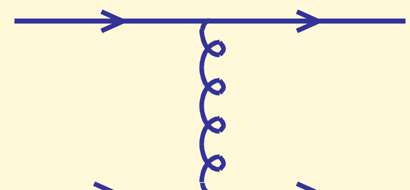

$q\bar{q} \to q\bar{q}$

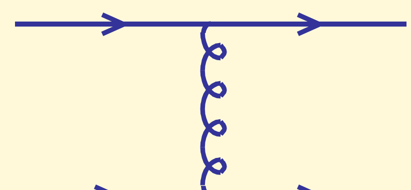

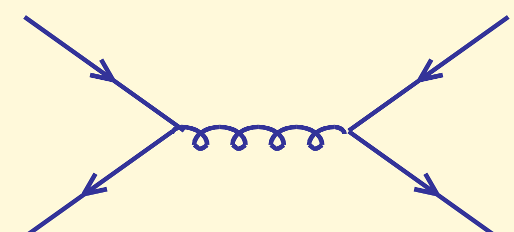

Phase space and cross-section for LO jet production

$$d[PS] = \frac{d^3p_1}{(2\pi)^2 2p_1^0}\frac{d^3p_2}{(2\pi)^2 2p_2^0}(2\pi)^4\delta^4(P_{in}-P_{out})\,dx_1\,dx_2$$

(a) $$\delta(E_{in}-E_{out})\,\delta(P^z_{in}-P^z_{out})\,dx_1\,dx_2 = \frac{1}{2E^2_{beam}}$$

(b) $$\frac{dp^z}{p^0} = dy \equiv d\eta$$

$$d[PS] = \frac{1}{4\pi S}\,p_T\,dp_T\,d\eta_1\,d\eta_2$$

$$\frac{d^3\sigma}{dp_T d\eta_1 d\eta_2} = \frac{p_T}{4\pi S}\sum_{i,j} f_i(x_1)\,f_j(x_2)\,\frac{1}{2\hat{s}}\overline{\sum_{kl}}|M(ij\to kl)|^2$$

The measurement of pT and rapidities for a dijet final state uniquely determines the parton momenta x_1 and x_2. Knowledge of the partonic cross-section allows therefore the determination of partonic densities f(x)

Small-angle jet production, a useful approximation for the determination of the matrix elements and of the cross-section

At small scattering angle, $t = (p_1 - p_3)^2 \sim (1 - \cos\theta) \to 0$

and the $1/t^2$ propagators associated with t-channel gluon exchange dominate the matrix elements for all processes. In this limit it is easy to evaluate the matrix elements. For example:

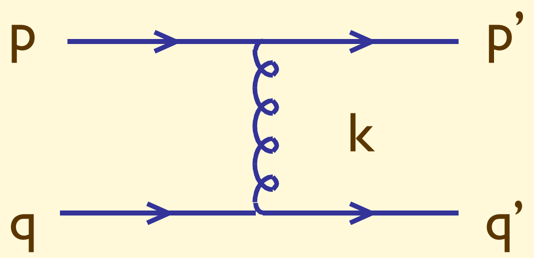

$$\sim (\lambda^a)_{ij} (\lambda^a)_{kl} (2p_\mu) \frac{1}{t} (2q_\mu) \;=\; \frac{2s}{t} (\lambda^a)_{ij} (\lambda^a)_{kl}$$

where we used the fact that, for k=p-p'<<p (small angle scattering),

$$u(p')\gamma_\mu u(p) \sim u(p)\gamma_\mu u(p) \;=\; 2p_\mu$$

Using our colour algebra results, we then get: $\overline{\sum_{col,spin}} |M|^2 = \frac{1}{N_c^2} \frac{N_c^2 - 1}{4} \frac{4s^2}{t^2}$

Noting that the result must be symmetric under s↔u exchange, and setting Nc=3, we finally obtain: $\overline{\sum_{col,spin}} |M|^2 = \frac{4}{9} \frac{s^2 + u^2}{t^2}$

which turns out to be the exact result!

Quark-gluon and gluon-gluon scattering

We repeat the exercise in the more complex case of qg scattering, assuming the dominance of the t-channel gluon-exchange diagram:

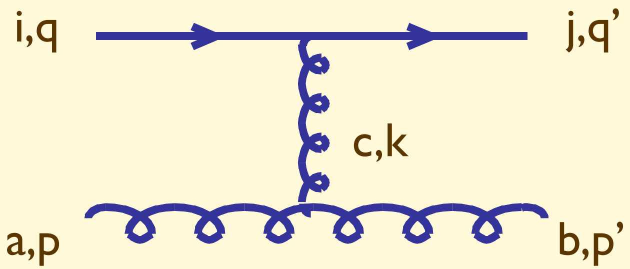

$$\sim f^{abc}\lambda^c_{ij}\, 2p_\mu \frac{1}{t} 2q_\mu \;=\; 2\frac{s}{t} f^{abc}\lambda^c_{ij}$$

Using the colour algebra results, and enforcing the s↔u symmetry, we get:

$$\overline{\sum_{col,spin}} |M|^2 = \frac{s^2+u^2}{t^2}$$

which differs by only 20% from the exact result

$$\overline{\sum_{col,spin}} |M|^2 = \frac{s^2+u^2}{t^2} - \frac{4}{9}\frac{s^2+u^2}{us}$$

even in the large-angle region, at 90°

In a similar way we obtain for gg scattering (using the t↔u symmetry):

$$\overline{\sum_{col,spin}} |M(gg \to gg)|^2 = \frac{9}{2}\left(\frac{s^2}{t^2} + \frac{s^2}{u^2}\right)$$

compared to the exact result

$$\overline{\sum_{col,spin}} |M(gg \to gg)|^2 = \frac{9}{2}\left(3 - \frac{ut}{s^2} - \frac{us}{t^2} - \frac{st}{u^2}\right)$$

with a 20% difference at 90°

Note that in the leading 1/t approximation we get the following result:

$$\hat{\sigma}_{gg} : \hat{\sigma}_{qg} : \hat{\sigma}_{qq} = \frac{9}{4} : 1 : \frac{4}{9}$$

where 4/9 = C_F / C_A = [(N^2-1)/2N] / N is the ratio of the squared colour charges of quarks and gluons

and therefore

$$d\sigma_{jet} = \int dx_1 dx_2 \sum_{ij} f_i(x_1) f_j(x_2) d\hat{\sigma}_{ij} = \int dx_1 dx_2 \sum_{ij} F(x_1) F(x_2) d\hat{\sigma}_{gg}$$

where we defined the `effective parton density' F(x):

$$F(x) = g(x) + \frac{4}{9} \sum_i [q_i(x) + q_i(x)]$$

As a result jet data cannot be used to extract separately gluon and quark densities. On the other hand, assuming an accurate knowledge of the quark densities (say from HERA), jet data can help in the determination of the gluon density

Process	$\frac{d\hat{\sigma}}{d\Phi_2}$	at 90°
$qq' \to qq'$	$\frac{4}{9}\frac{\hat{s}^2+\hat{u}^2}{\hat{t}^2}$	2.22
$qq \to qq$	$\left[\frac{4}{9}\left(\frac{\hat{s}^2+\hat{u}^2}{\hat{t}^2}+\frac{\hat{s}^2+\hat{t}^2}{\hat{u}^2}\right)-\frac{8}{27}\frac{\hat{s}^2}{\hat{u}\hat{t}}\right]$	3.26
$q\bar{q} \to q'\bar{q}'$	$\frac{4}{9}\frac{\hat{t}^2+\hat{u}^2}{\hat{s}^2}$	0.22
$q\bar{q} \to q\bar{q}$	$\left[\frac{4}{9}\left(\frac{\hat{s}^2+\hat{u}^2}{\hat{t}^2}+\frac{\hat{t}^2+\hat{u}^2}{\hat{s}^2}\right)-\frac{8}{27}\frac{\hat{u}^2}{\hat{s}\hat{t}}\right]$	2.59
$q\bar{q} \to gg$	$\left[\frac{32}{27}\frac{\hat{t}^2+\hat{u}^2}{\hat{t}\hat{u}}-\frac{8}{3}\frac{\hat{t}^2+\hat{u}^2}{\hat{s}^2}\right]$	1.04
$gg \to q\bar{q}$	$\left[\frac{1}{6}\frac{\hat{t}^2+\hat{u}^2}{\hat{t}\hat{u}}-\frac{3}{8}\frac{\hat{t}^2+\hat{u}^2}{\hat{s}^2}\right]$	0.15
$gq \to gq$	$\left[-\frac{4}{9}\frac{\hat{s}^2+\hat{u}^2}{\hat{s}\hat{u}}+\frac{\hat{u}^2+\hat{s}^2}{\hat{t}^2}\right]$	6.11
$gg \to gg$	$\frac{9}{2}\left(3-\frac{\hat{t}\hat{u}}{\hat{s}^2}-\frac{\hat{s}\hat{u}}{\hat{t}^2}-\frac{\hat{s}\hat{t}}{\hat{u}^2}\right)$	30.4